

## Synthesis and Characterization of Oxidized $W_6S_8L_6$ Clusters

Laurie I. Hill, Song Jin, Ran Zhou, D. Venkataraman, and Francis J. DiSalvo<sup>\*,†</sup>

Baker Laboratories, Department of Chemistry and Chemical Biology, Cornell University, Ithaca, New York 14853

Received October 3, 2000

Cationic  $[W_6S_8L_6]PF_6$  ( $L = PEt_3$  (**3**), 4-*tert*-butylpyridine (**4**)) clusters were successfully synthesized and isolated for the first time by reacting the corresponding neutral  $W_6S_8L_6$  ( $L = PEt_3$  (**1**), 4-*tert*-butylpyridine (**2**)) clusters with  $[Cp_2Fe]PF_6$  as the oxidant. The products **3** and **4** were characterized by NMR spectroscopy, mass spectroscopy, and X-ray crystallography (only for **3**) and shown to be the desired oxidized  $W_6S_8$  clusters with a metal electron count of 19. Magnetic property studies showed that they are paramagnetic compounds with  $S = 1/2$ . Their chemical properties and stability are also reported. Crystal data for **3**·2THF: space group,  $R\bar{3}$  (No. 148);  $a = 13.91170(10)$  Å;  $c = 32.4106(2)$  Å;  $Z = 3$ .

### Introduction

Octahedral molybdenum clusters of the formula  $Mo_6Q_8$  ( $Q = S, Se, Te$ ) are the building blocks of a class of compounds known as Chevrel phases,<sup>1,2</sup> which have been extensively studied due to their interesting properties such as superconductivity,<sup>3</sup> fast ion conductivity,<sup>4</sup> and hydrodesulfurization catalytic activity.<sup>5–8</sup> Since the pioneering work by Saito and co-workers,<sup>9</sup> many molecular octahedral clusters  $M_6Q_8$  ( $M = Cr, Mo, W$ ;  $Q = S, Se, Te$ ) similar to those present in Chevrel phases have been synthesized.<sup>10–21</sup> Although many have tried to use the

molecular Cr and W octahedral clusters as precursors for the corresponding chromium and tungsten “Chevrel phases”, unknown from solid-state routes, no reports of success are known to us.<sup>14,15,18,22,23</sup>

We are interested in using the molecular compounds  $W_6S_8L_6$  ( $L$  is a Lewis base ligand) as precursors to cluster networks linked by  $\pi$ -conjugated ditopic ligands.<sup>20,21</sup> Extended Hückel calculations<sup>24</sup> performed on “bare”  $W_6S_8$  clusters indicate that neutral clusters have a metal electron count (MEC) of 20. Their highest occupied molecular orbital (HOMO) is triply degenerate and composed of metal d-orbitals of the appropriate symmetry to interact with the  $\pi$ -orbitals of an organic ligand. Therefore, intercluster interaction within the extended network is possible. However, the full HOMO of the cluster at a MEC of 20 would lead to a filled band at the Fermi level of the extended network and result in semiconducting behavior. A network built of clusters with a MEC of 18 or 19 would lead to a partially filled band and a potentially conducting network. The HOMO of clusters with higher MECs of 21–24 has  $\delta$  symmetry with respect to the M–L axis, and thus these clusters are inappropriate for significant intercluster interactions through organic ligands. In anticipation of building an extended network of clusters with a MEC below 20, we have pursued the synthesis of oxidized  $W_6S_8L_6$  ( $L = PEt_3$ , 4-*tert*-butylpyridine) clusters.

While reduced  $M_6Q_8L_6$  ( $M = Mo$ ;  $Q = S, Se$ ;<sup>11,25</sup> and  $M = W$ ;  $Q = Te$ <sup>18</sup>) clusters with a MEC of 21 electrons have been synthesized and characterized, no oxidized  $M_6Q_8L_6$  clusters with a MEC of 19 electrons have been reported. However, on the basis of the electrochemical studies of  $W_6S_8L_6$  clusters carried out by this<sup>20</sup> and other groups,<sup>10</sup> it seemed likely that stable oxidized clusters could be prepared by chemical methods. We report herein the synthesis and isolation of the first cationic  $[W_6S_8L_6]PF_6$  ( $L = PEt_3$  (**3**), 4-*tert*-butylpyridine (**4**)) clusters with a MEC of 19 using  $[Cp_2Fe]PF_6$  ( $Cp = C_5H_5$ , cyclopentadienyl) as the oxidant. These compounds were characterized

<sup>†</sup> E-mail: fjd3@cornell.edu.

- (1) Chevrel, R.; Sergent, M.; Prigent, J. *J. Solid State Chem.* **1971**, *3*, 515–519.
- (2) Pena, O.; Sergent, M. *Prog. Solid State Chem.* **1989**, *19*, 165–281.
- (3) *Topics in Current Physics*, Vol. 34: Superconductivity in Ternary Compounds 2: Superconductivity and Magnetism; Maple, M. B., Fischer, Ø., Eds.; Springer-Verlag: Heidelberg, 1982.
- (4) Mulhern, P. J.; Haering, R. R. *Can. J. Phys.* **1984**, *62*, 527–531.
- (5) McCarty, K. F.; Schrader, G. L. *Ind. Eng. Chem. Prod. Res. Dev.* **1984**, *23*, 519–524.
- (6) McCarty, K. F.; Andereg, J. W.; Schrader, G. L. *J. Catal.* **1985**, *93*, 375–387.
- (7) Hilsenbeck, S. J.; McCarley, R. E.; Thompson, R. K.; Flanagan, L. C.; Schrader, G. L. *J. Mol. Catal. A* **1997**, *122*, 13–24.
- (8) Hilsenbeck, S. J.; McCarley, R. E.; Goldman, A. I.; Schrader, G. L. *Chem. Mater.* **1998**, *10*, 125–134.
- (9) Saito, T.; Yamamoto, N.; Yamagata, T.; Imoto, H. *J. Am. Chem. Soc.* **1988**, *110*, 1646–1647.
- (10) Saito, T.; Yoshikawa, A.; Yamagata, T. *Inorg. Chem.* **1989**, *28*, 3588–3592.
- (11) Saito, T.; Yamamoto, N.; Nagase, T.; Tsuboi, T.; Kobayashi, K.; Yamagata, T.; Imoto, H.; Unoura, K. *Inorg. Chem.* **1990**, *29*, 764–770.
- (12) Hilsenbeck, S. J.; Young, V. G., Jr.; McCarley, R. E. *Inorg. Chem.* **1994**, *33*, 1822–1832.
- (13) Ehrlich, G. M.; Warren, C. J.; Vennos, D. A.; Ho, D. M.; Haushalter, R. C.; DiSalvo, F. J. *Inorg. Chem.* **1995**, *34*, 4454–4459.
- (14) Xie, X. B.; McCarley, R. E. *Inorg. Chem.* **1995**, *34*, 6124–6129.
- (15) Zhang, X.; McCarley, R. E. *Inorg. Chem.* **1995**, *34*, 2678–2683.
- (16) Tsuge, K.; Imoto, H.; Saito, T. *Bull. Chem. Soc. Jpn.* **1996**, *69*, 627–636.
- (17) Xie, X. B.; McCarley, R. E. *Inorg. Chem.* **1996**, *35*, 2713–2714.
- (18) Xie, X. B.; McCarley, R. E. *Inorg. Chem.* **1997**, *36*, 4665–4675.
- (19) Kamiguchi, S.; Imoto, H.; Saito, T.; Chihara, T. *Inorg. Chem.* **1998**, *37*, 6852–6857.
- (20) Venkataraman, D.; Rayburn, L. L.; Hill, L. I.; Jin, S.; Malik, A.-S.; Turneau, K. J.; DiSalvo, F. J. *Inorg. Chem.* **1999**, *38*, 828–830.
- (21) Jin, S.; Venkataraman, D.; DiSalvo, F. J. *Inorg. Chem.* **2000**, *39*, 2747–2757.

- (22) Hilsenbeck, S. J.; McCarley, R. E.; Goldman, A. I. *Chem. Mater.* **1995**, *7*, 499–506.
- (23) McCarley, R. E.; Hilsenbeck, S. J.; Xie, X. *J. Solid State Chem.* **1995**, *117*, 269–274.
- (24) Malik, A.-S. Ph.D. Thesis, Cornell University, Ithaca, NY, 1998.
- (25) Mizutani, J.; Amari, S.; Imoto, H.; Saito, T. *J. Chem. Soc., Dalton Trans.* **1998**, 819–824.

by X-ray crystallography (only for **3**), NMR spectroscopy, mass spectroscopy, and magnetic susceptibility.

### Experimental Section

**General.** W<sub>6</sub>S<sub>8</sub>(PEt<sub>3</sub>)<sub>6</sub> (**1**) and W<sub>6</sub>S<sub>8</sub>(4-*tert*-butylpyridine)<sub>6</sub> (**2**) were synthesized according to previously reported procedures.<sup>20</sup> Ferrocenium hexafluorophosphate ([Cp<sub>2</sub>Fe]PF<sub>6</sub>) from Aldrich was recrystallized from acetonitrile. *N,N*-Dimethylformamide (DMF), dichloromethane (CH<sub>2</sub>Cl<sub>2</sub>), and acetonitrile were dried over 4 Å molecular sieves and distilled under reduced pressure. Tetrahydrofuran (THF), benzene, and diethyl ether were treated with sodium wire and distilled under reduced pressure. All reactants and solvents were stored in a glovebox filled with argon. All glassware was flame dried before use. All manipulations were carried out in the glovebox or using standard Schlenk techniques unless otherwise noted.

<sup>1</sup>H NMR spectra were obtained in CD<sub>2</sub>Cl<sub>2</sub> on a Varian INOVA 400 spectrometer with no <sup>31</sup>P decoupling and were referenced to internal residual solvent resonances. <sup>31</sup>P NMR spectra were obtained in CD<sub>2</sub>Cl<sub>2</sub> using a Varian VXR-400 spectrometer at 162 MHz with 85% H<sub>3</sub>PO<sub>4</sub> as an external standard and with <sup>1</sup>H decoupling. High-resolution ESI-MS data were collected with CH<sub>2</sub>Cl<sub>2</sub> solution of the products using a Micromass LCT mass spectrometer in the positive ion mode.

**Synthesis of [W<sub>6</sub>S<sub>8</sub>(PEt<sub>3</sub>)<sub>6</sub>]PF<sub>6</sub> (**3**). Method A.** In a 100 mL Schlenk flask equipped with a Teflon stir bar, **1** (0.200 g, 0.097 mmol) was dissolved into 50 mL of CH<sub>2</sub>Cl<sub>2</sub> to form a dark yellow-brown solution. A blue solution of [Cp<sub>2</sub>Fe]PF<sub>6</sub> (0.035 g, 0.106 mmol) in 20 mL of CH<sub>2</sub>Cl<sub>2</sub> was added to the flask. The resulting green solution was stirred for 30 min before the solvent was removed under dynamic vacuum. The resulting green residue was washed repeatedly with benzene and then with diethyl ether. The dried green powder of **3** weighed 0.184 g (85% yield).

**Method B.** [Cp<sub>2</sub>Fe]PF<sub>6</sub> (0.066 g, 0.199 mmol) was added into a solution of W<sub>6</sub>S<sub>8</sub>(PEt)<sub>6</sub> (0.114 g, 0.055 mmol) in 20 mL of benzene. Upon stirring, the color of the solution changed from yellow to green within an hour, accompanied by some precipitation. After 2 days, the green precipitate was filtered, washed with diethyl ether, and allowed to dry. The yield of **3** was 0.116 g (95%).

Samples of **3** from both methods gave the following. <sup>1</sup>H NMR: δ 1.5 (t, 3, Me) and 4.0 (q, 2, CH<sub>2</sub>). <sup>31</sup>P{<sup>1</sup>H} NMR: δ -143 (septet, <sup>1</sup>J<sub>F-P</sub> = 715 Hz); -419 (broad hump). ESI-MS: *m/z* obsd (calcd) 2067.98 (2068.02).

**Synthesis of [W<sub>6</sub>S<sub>8</sub>(4-*tert*-butylpyridine)<sub>6</sub>]PF<sub>6</sub> (**4**). Method A.** In a 100 mL Schlenk flask equipped with a Teflon stir bar, **2** (0.200 g, 0.092 mmol) was dissolved into 75 mL of CH<sub>2</sub>Cl<sub>2</sub> to form a dark orange solution. A solution of [Cp<sub>2</sub>Fe]PF<sub>6</sub> (0.034 g, 0.101 mmol) in 20 mL of CH<sub>2</sub>Cl<sub>2</sub> was added to the flask to result in a green-brown solution. After stirring for 30 min, the solvent was removed by dynamic vacuum. The resulting green solid was washed repeatedly with benzene until the filtrate no longer became colored. After washing with diethyl ether, the dried green powder weighed 0.150 g (70% yield).

**Method B.** [Cp<sub>2</sub>Fe]PF<sub>6</sub> (0.054 g, 0.163 mmol) was added into a solution of W<sub>6</sub>S<sub>8</sub>(4-*tert*-butylpyridine)<sub>6</sub> (0.119 g, 0.055 mmol) in 20 mL of benzene. Upon stirring, the color of solution changed from dark orange to green within an hour. After 2 days, the green precipitate was filtered, washed with diethyl ether, and allowed to dry. The yield of **4** was 0.106 g (83%).

Samples of **4** from both methods gave the following. <sup>1</sup>H NMR: δ 1.5 (s, 9, Me), 6.43 (broad doublet, 2, β-H), and 8.38 (broad doublet, 2, α-H). <sup>31</sup>P{<sup>1</sup>H} NMR: δ -143 (septet, <sup>1</sup>J<sub>F-P</sub> = 715 Hz). ESI-MS: *m/z* obsd (calcd) 2170.01 (2170.10).

**X-ray Crystallographic Study of [W<sub>6</sub>S<sub>8</sub>(PEt<sub>3</sub>)<sub>6</sub>]PF<sub>6</sub>.** Single crystals suitable for X-ray studies were grown from a THF/CH<sub>2</sub>Cl<sub>2</sub> solution of **3** by slow removal of the solvent. Most of the crystals formed as roughly square thin green plates. A green block-shaped crystal measuring 0.15 × 0.1 × 0.1 mm was mounted on a plastic loop with polybutylene oil and immediately placed in a cold dinitrogen stream. X-ray intensity data were collected using Mo Kα radiation at -110 °C on a Bruker SMART diffractometer with a CCD detector. The cell constants were determined from more than 50 centered reflections as rhombohedral with lattice parameters *a* = 13.4621(1) Å, α = 62.222(1)° or in

**Table 1.** Crystallographic Data for [W<sub>6</sub>S<sub>8</sub>(PEt<sub>3</sub>)<sub>6</sub>]PF<sub>6</sub>·2THF

3·2THF	
chem formula	C <sub>44</sub> H <sub>90</sub> F <sub>6</sub> O <sub>2</sub> P <sub>7</sub> S <sub>8</sub> W <sub>6</sub>
fw	2341.53
space group	R $\bar{3}$ (No. 148)
<i>a</i> , Å	13.91170(10)
<i>c</i> , Å	32.4106(2)
<i>V</i> , Å <sup>3</sup>	5432.23(6)
<i>Z</i>	3
temp, °C	-110
λ, Å	0.710 73
ρ <sub>calcd</sub> , g cm <sup>-3</sup>	2.147
μ, cm <sup>-1</sup>	99.22
<i>R</i> <sub>1</sub> <sup>a</sup> ( <i>I</i> > 2σ/all)	0.0451/0.0755
<i>wR</i> <sub>2</sub> <sup>b</sup> ( <i>I</i> > 2σ/all)	0.0539/0.0774

$$^a R_1 = \sum ||F_o| - |F_c|| / \sum |F_o|. \quad ^b wR_2 = [\sum w(F_o^2 - F_c^2)^2 / \sum w(F_o^2)^2]^{1/2}.$$

hexagonal setting, *a* = 13.9117(10) Å, *c* = 32.4106(2) Å. The space group (R $\bar{3}$ , No. 148) was determined on the basis of systematic absences and intensity statistics. A total of 11328 reflections were collected in the θ range 1.8 to 28.9°, 2723 of which were unique. The data were integrated using SAINT software, and an empirical absorption correction was applied using the program SADABS.<sup>26</sup> The structure was solved using SHELXS and refined using full-matrix least-squares method on *F*<sub>o</sub><sup>2</sup> with SHELXL software packages.<sup>27</sup> PF<sub>6</sub><sup>-</sup> anions were modeled as disordered such that the four F atoms on sites F(2) and F(3) perpendicular to the three-fold axis occupy three different positions at 1/3 occupancy. The solvent THF molecules were modeled as disordered in three different planar orientations (perpendicular to the 3-fold axis) such that the O atom site had an occupancy of 1/3 and the two C atom sites each had an occupancy of 2/3. Additionally, the ethyl groups of the PEt<sub>3</sub> ligands were modeled as disordered and refined such that each C atom site had an occupancy of approximately 1/2. Although it is likely that the pseudosymmetry of the heavy cluster core could dominate the symmetry of the full structure, attempts to refine the structure with lower symmetry or twinning have so far been unsuccessful. Also, possible superlattices could not be detected in this data set. Hydrogen atoms were added at calculated fixed positions. W, S, and P atoms were refined anisotropically. All other non-hydrogen atoms were refined isotropically. Final refinements converged and gave satisfactory residue factors. The largest residual electron densities were close to W atoms. Details of the crystallographic data are given in Table 1, selected bond distances and angles, in comparison with those found in 1·2C<sub>6</sub>H<sub>6</sub>,<sup>20</sup> are given in Table 2.

**Magnetic Susceptibility.** Under an argon atmosphere, 80.1 mg of **3** was loaded into a gelcap. The gelcap was inserted into a straw which was then placed into a Quantum Design SQUID magnetometer with minimal exposure to air. Magnetic susceptibility measurements were carried out over the temperature range 4–300 K with an applied field of 7000 Oe. The susceptibility at 300 K as a function of field (100–10000 Oe) was also measured to check for ferromagnetic impurities. A measurement was performed on **4** (52.1 mg) in the same fashion except that the applied magnetic field was 1000 Oe. The data were corrected for small ferromagnetic impurities and also for the diamagnetic core contributions (-1.14 × 10<sup>-3</sup> emu/mol for **3** and -1.18 × 10<sup>-3</sup> emu/mol for **4**) which were calculated from values for the individual atoms.<sup>28</sup>

**ESR Study.** Solid samples of compound **3** were loaded into ESR tubes under an argon atmosphere. The ESR spectra were obtained at a frequency of 9.55 GHz on a Bruker ER-200 ESR spectrometer at liquid nitrogen temperature.

**Thermogravimetric Analyses (TGA).** Thermogravimetric analyses (TGA) of **3** and **4** were carried out on a Seiko TG/DTA 220 thermal

(26) Sheldrick, G. M. *the computer program SADABS is used by Siemens CCD diffractometers*; Institute für Anorganische Chemie der Universität Göttingen.

(27) Sheldrick, G. M. *SHELXL*, 5.03 ed.; Siemens Analytical X-ray Instruments Inc.: Madison, WI, 1994.

(28) Selwood, P. W. *Magnetochemistry*, 2nd ed.; Interscience: New York, 1956; p 78.

**Table 2.** Selected Bond Lengths [Å] and Angles [deg] for **3** and **1**<sup>a</sup>

	3	1
W(1)–W(1)A	2.6803(4)	2.6813(6)
W(1)–W(1)B	2.6809(3)	2.6759(6)
mean W–W	2.6806(4)	2.6786(6)
W(1)–S(1)	2.456(2)	2.458(2)
W(1)–S(2)	2.449(2)	2.4585(18)
W(1)–S(2)A	2.446(2)	2.4511(17)
W(1)–S(2)B	2.4508(15)	2.4556(17)
mean W–S	2.450(2)	2.456(2)
W(1)–P(1)	2.530(2)	2.5230(18)
W(1)A–W(1)–W(1)B <sup>b</sup>	60.006(5)	59.931(8)
W(1)B–W(1)–W(1)D	59.985(10)	60.134(17)
W(1)C–W(1)–W(1)D	60.007(5)	59.931(8)

<sup>a</sup> Both clusters crystallized in the same  $R\bar{3}$  space group. Data for **1** were taken from ref 20. Symmetry transformations used to generate equivalent atoms: A,  $-x + y, -x + 1, z$ ; B,  $y - 1/3, -x + y + 1/3, -z + 1/3$ ; C,  $-y + 1, x - y + 1, z$ ; D,  $x - y + 2/3, x + 1/3, -z + 1/3$ .<sup>b</sup> As required by the imposed symmetry, W–W–W angles within all equatorial squares are 90° and W–W–W angles within those triangular faces perpendicular to the three-fold axes are 60°. The mean angles within triangular faces are 60° by geometry.

analyzer. The samples were loaded in air into an aluminum pan and were heated from room temperature to 550 °C at the rate of 20 °C/min under a flow of dinitrogen (60 mL/min).

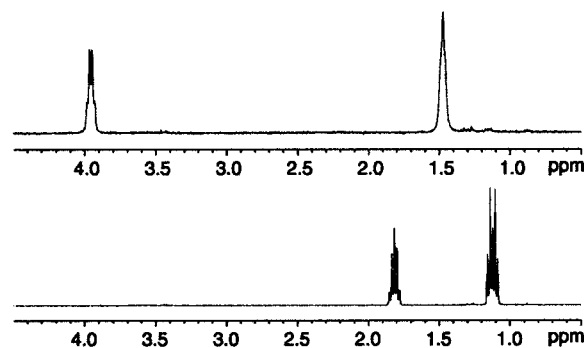
## Results and Discussion

**Synthesis and Isolation of [W<sub>6</sub>S<sub>8</sub>L<sub>6</sub>]PF<sub>6</sub> (**3**).** A few factors were considered when choosing the oxidizing agent(s) for the synthesis of the oxidized clusters. First, according to our cyclic voltammetry studies,<sup>20</sup> the oxidizing agent needs to have a standard reduction potential larger than 0.2 V but less than 0.6 V, beyond which possible irreversible oxidation occurs. With the electrochemistry of ferrocenium well understood and its use as an oxidizing agent well documented,<sup>29</sup> [Cp<sub>2</sub>Fe]PF<sub>6</sub> was found to meet this criterion. Upon the addition of more than 1 equiv of [Cp<sub>2</sub>Fe]PF<sub>6</sub>, the color of the W<sub>6</sub>S<sub>8</sub>L<sub>6</sub> solution in CH<sub>2</sub>Cl<sub>2</sub> instantaneously changed to green. The reaction involved is



It is also important that the reduction byproduct, i.e., Cp<sub>2</sub>Fe, is inert to further reaction with the oxidized clusters and easy to remove from the product mixture. Cp<sub>2</sub>Fe is soluble in benzene, while the oxidized clusters are soluble in polar solvents such as CH<sub>2</sub>Cl<sub>2</sub>, benzonitrile, acetonitrile, DMF, acetone, and THF but only sparingly soluble in benzene and not soluble in Et<sub>2</sub>O and heptane. Other complicating factors include the stability of the products **3** and **4** in different solvents (vide infra).

These factors are the basis of the methods reported. In method A, the Cp<sub>2</sub>Fe byproduct was easily removed with benzene. In method B, the oxidized clusters precipitated out since they are only sparingly soluble in benzene, while other byproducts or unreacted species were left behind in the benzene solution. In both methods, a wash with Et<sub>2</sub>O removed unreacted [Cp<sub>2</sub>Fe]PF<sub>6</sub>, which is especially important in method B. The advantage of method A is the fast reaction facilitated by the good solubility of both reactants in CH<sub>2</sub>Cl<sub>2</sub>—allowing the solution to stand for longer periods of time (>6 h) did not have any effect on the

**Figure 1.** <sup>1</sup>H NMR spectra (0–4.5 ppm regions) of [W<sub>6</sub>S<sub>8</sub>(PEt<sub>3</sub>)<sub>6</sub>]PF<sub>6</sub> (top) and W<sub>6</sub>S<sub>8</sub>(PEt<sub>3</sub>)<sub>6</sub> (bottom) in CD<sub>2</sub>Cl<sub>2</sub>.

results. Method B is simpler and consumes less solvent, but a prolonged reaction time (>2 d) is essential for good yields. This slow reaction is likely due to the limited solubility of [Cp<sub>2</sub>Fe]PF<sub>6</sub> in benzene.

**<sup>1</sup>H and <sup>31</sup>P NMR Spectroscopy of [W<sub>6</sub>S<sub>8</sub>L<sub>6</sub>]PF<sub>6</sub>.** The <sup>1</sup>H NMR spectrum of **3** in CD<sub>2</sub>Cl<sub>2</sub> is shown in Figure 1 (top) in comparison with that of **1** (bottom). The <sup>1</sup>H resonances for the oxidized cluster **3** are shifted downfield from those of the neutral cluster **1** to δ 1.50 (Me) and 4.00 (CH<sub>2</sub>),<sup>20</sup> consistent with the increased electron-withdrawing effect by the cationic cluster. The signals for **3** are significantly broadened, owing to the paramagnetic cluster core (vide infra). Interestingly, the coupling with <sup>31</sup>P is no longer observable in the oxidized cluster and the <sup>1</sup>H NMR peaks appear as a triplet and a quartet, in contrast to the multiplets observed for **1** and free PEt<sub>3</sub>. This type of behavior has also been found in [Co<sub>6</sub>S<sub>8</sub>(PEt<sub>3</sub>)<sub>6</sub>]<sup>+1,+2</sup> and [Co<sub>6</sub>Te<sub>8</sub>(PEt<sub>3</sub>)<sub>6</sub>]<sup>0,+1</sup>.<sup>30–32</sup> The <sup>31</sup>P NMR spectrum for **3** consists of a septet centered at δ –143 due to PF<sub>6</sub><sup>–</sup> (reported value δ –145<sup>33</sup>) and a very broad signal at about δ –419 which is tentatively assigned to the PEt<sub>3</sub> bound to the oxidized cluster (δ –19.2 for free PEt<sub>3</sub> and δ –16.97 for PEt<sub>3</sub> bound to neutral cluster<sup>34</sup>). The discrepancy between the observed integration ratio of PEt<sub>3</sub> to PF<sub>6</sub><sup>–</sup> (2.6 to 1) and the expected ratio of 6 to 1 is attributed to the paramagnetic nature of **3**.

The <sup>1</sup>H NMR spectrum of **4** in CD<sub>2</sub>Cl<sub>2</sub>, of which the downfield region is shown in Figure 2 (top) along with that of **2** (bottom), consists of two equally intense broadened (due to the paramagnetic cluster) doublets at δ 8.38 (α-H) and 6.43 (β-H). These are shifted *upfield* from the <sup>1</sup>H signals of the 4-*tert*-butylpyridine bound to the neutral W<sub>6</sub>S<sub>8</sub> cluster (δ 9.20 for α-H and 7.30 for β-H)<sup>20</sup> and those of free 4-*tert*-butylpyridine in CD<sub>2</sub>Cl<sub>2</sub> (δ 8.46 for α-H and 7.28 for β-H). These *upfield* shifts are in contrast to the *downfield* shifts for PEt<sub>3</sub> in **3** and for the methyl proton in the same cluster **4** (from δ 1.30 in **2** to 1.50 in **4**). This is also contrary to the shifts of pyridine protons found in most paramagnetic transition metal complexes, which show an alternation of upfield and downfield shifts around the ring, attributed to spin delocalization via the pyridine ring.<sup>35</sup> These

(29) See for example: Page, J. A.; Wilkinson, G. *J. Am. Chem. Soc.* **1952**, *74*, 6149. Kuwana, T.; Bublitz, D. E.; Hoh, G. *J. Am. Chem. Soc.* **1960**, *82*, 5811. Ge, Y.-W.; Ye, Y.; Sharp, P. R. *J. Am. Chem. Soc.* **1994**, *116*, 8384–8385. Westerberg, D. E.; Pladzewicz, J. R.; Abrahamson, A. J.; Davis, R. A.; Likar, M. D. *Inorg. Chem.* **1987**, *26*, 2058.

(30) Bencini, A.; Midollini, S.; Zanchini, C. *Inorg. Chem.* **1992**, *31*, 2132–2137.  
 (31) Ceconi, F.; Ghilardi, C. A.; Midollini, S.; Orlandini, A.; Zanello, P.; Cingantini, A.; Bencini, A.; Uytterhoeven, M. G.; Giorgi, G. *J. Chem. Soc., Dalton Trans.* **1995**, 3881–3890.  
 (32) Ceconi, F.; Ghilardi, C. A.; Midollini, S.; Orlandini, A.; Bencini, A. *J. Chem. Soc., Dalton Trans.* **1996**, 3991–3994.  
 (33) *Multinuclear NMR*; Mason, J., Ed.; Plenum Press: New York, 1987.  
 (34) Jin, S.; DiSalvo, F. J., unpublished result.  
 (35) See for example: Pearson, C.; Beauchamp, A. L. *Can. J. Chem.* **1997**, *75*, 220. Miller, R. G.; Stauffer, R. D.; Fahey, D. R.; Parnell, D. R. *J. Am. Chem. Soc.* **1970**, *92*, 1511. Happe, J. A.; Ward, R. L. *J. Chem. Phys.* **1963**, *39*, 1211.

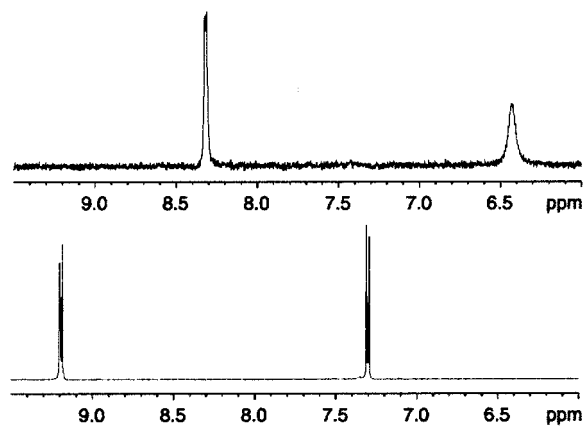


**Figure 2.** <sup>1</sup>H NMR spectra (6–10 ppm regions) of [W<sub>6</sub>S<sub>8</sub>(4-*tert*-butylpyridine)<sub>6</sub>]PF<sub>6</sub> (top) and W<sub>6</sub>S<sub>8</sub>(4-*tert*-butylpyridine)<sub>6</sub> (bottom) in CD<sub>2</sub>Cl<sub>2</sub>.

seemingly opposite shifts in **4** can be explained by the combination of two competing electron density effects on the chemical shifts of the protons on the aromatic ligand.<sup>36</sup> One effect is the electron-withdrawing effect, which shifts resonances *downfield* when electron density is withdrawn. The other is the ring current effect, which shifts resonances *upfield* when electron density is withdrawn from the ring. When 4-*tert*-butylpyridine is bound to the neutral cluster, the electron-withdrawing effect must be the dominant effect and results in downfield shifts compared to those of the free ligand. However, the main effect incurred on oxidation is the ring current effect, evidenced by the similar shifts of both aromatic protons from the positions in the neutral cluster, since all ring protons are expected to be affected in the same way. The electron-withdrawing effect is still present, affecting mostly the  $\alpha$ -H. The methyl protons are primarily affected by the greater electron-withdrawing effect from the pyridine ring as a result of lower ring current and thus are shifted downfield.

The <sup>31</sup>P NMR spectrum of **4** only consists of one septet corresponding to PF<sub>6</sub><sup>−</sup>, which, combined with the absence of [Cp<sub>2</sub>Fe]<sup>+</sup> by <sup>1</sup>H NMR and microprobe analysis, further supports the fact that the W<sub>6</sub>S<sub>8</sub>(4-*tbp*)<sub>6</sub> cluster is indeed oxidized. The purity of both **3** and **4** is evident in the absence of any extraneous peaks in the <sup>1</sup>H NMR spectra.

**Crystal Structure of [W<sub>6</sub>S<sub>8</sub>(PEt<sub>3</sub>)<sub>6</sub>]PF<sub>6</sub>·2THF.** X-ray structure analysis confirmed that cluster **3** was the oxidized cationic cluster as proposed. **3**·2THF crystallizes in the space group *R* $\bar{3}$  with *Z* = 3. Figure 3 shows the hexagonal arrangement of the [W<sub>6</sub>S<sub>8</sub>(PEt<sub>3</sub>)<sub>6</sub>]<sup>+</sup> ions located in planes perpendicular to the *c*-axis. Both the [W<sub>6</sub>S<sub>8</sub>(PEt<sub>3</sub>)<sub>6</sub>]<sup>+</sup> clusters and the PF<sub>6</sub><sup>−</sup> anions are centered on special positions with  $\bar{3}$  symmetry (*3b* and *3a* positions, respectively). The disordered THF molecules are centered on positions with  $\bar{3}$  symmetry (*6c* position). The packing of these moieties can be understood in terms of the “sphere” packing of clusters. The [W<sub>6</sub>S<sub>8</sub>(PEt<sub>3</sub>)<sub>6</sub>]<sup>+</sup> clusters approximately form ABCABC... close packed layers perpendicular to the *c*-axis; all octahedral holes in this array are occupied by PF<sub>6</sub><sup>−</sup> anions and all tetrahedral holes are occupied by the disordered THF molecules.

The [W<sub>6</sub>S<sub>8</sub>(PEt<sub>3</sub>)<sub>6</sub>]<sup>+</sup> cationic cluster has an imposed  $\bar{3}$  symmetry. The average W–W distance in **3** is 2.6806(4) Å, slightly longer than that in the neutral cluster **1**, 2.6786(6) Å,<sup>20</sup> but within 2 $\sigma$ . This difference is insignificant. A slightly longer

W–W bond length in the oxidized clusters is to be expected, since one electron is removed from a *slightly* bonding orbital<sup>24</sup> leading to weaker bonding. However, this effect is expected to be small, as observed here, since only one electron out of 20 is removed. This change is quite small compared with the change made by adding one electron to neutral clusters, as observed in [Mo<sub>6</sub>Q<sub>8</sub>(PET<sub>3</sub>)<sub>6</sub>]<sup>−</sup> (Q = S, Se) (0.010 Å elongation)<sup>11</sup> and [W<sub>6</sub>Te<sub>8</sub>(py)<sub>6</sub>]<sup>−</sup> (0.017 Å shortening).<sup>18</sup> The regular octahedron of W atoms found in **3** is in contrast to the tetragonally distorted octahedra found in the group VI clusters with a MEC of 21, [Mo<sub>6</sub>Q<sub>8</sub>(PET<sub>3</sub>)<sub>6</sub>]<sup>−</sup> (Q = S, Se)<sup>11</sup> and [W<sub>6</sub>Te<sub>8</sub>(py)<sub>6</sub>]<sup>−</sup>,<sup>18</sup> which has been attributed to the Jahn–Teller effect resulting from the partially filled degenerate e<sub>g</sub> HOMO orbitals in those clusters. Similar distortions have also been found in the clusters with a MEC of 19, Nb<sub>6</sub>I<sub>11</sub> (Nb<sub>6</sub>I<sub>8</sub>I<sub>6/2</sub><sup>a-a</sup>) (Nb–Nb = 2.72–2.96 Å) and Nb<sub>6</sub>I<sub>9</sub>S (Nb<sub>6</sub>I<sub>6</sub><sup>i</sup>S<sub>2/2</sub><sup>i-i</sup>I<sub>6/2</sub><sup>a-a</sup>) (Nb–Nb = 2.80–3.16 Å),<sup>37</sup> which have been attributed to a Jahn–Teller effect resulting from the partially filled degenerate t<sub>2g</sub> HOMO orbitals. However, the “strain” caused by the connectivity between the clusters can also lead to the distortions,<sup>38</sup> an explanation supported by the fact that similar distortions were observed in the clusters HNb<sub>6</sub>I<sub>11</sub> (Nb–Nb = 2.806–2.950 Å), CsNb<sub>6</sub>I<sub>11</sub> (Nb–Nb = 2.771–2.940 Å), and HNb<sub>6</sub>I<sub>9</sub>S (Nb–Nb = 2.888–3.014 Å)<sup>39</sup> which have a MEC of 20 but the same connectivity as the 19 electron clusters.

The W–P bond length in **3** compared to that in the neutral cluster **1** is of particular interest to us. A decrease in bond length on oxidation would likely lead to greater overlap between the orbitals which is important to an extended, conducting network because it would lead to a more disperse band at the Fermi level and increase the probability of obtaining a conducting system. In the case at hand, the average W–P bond length slightly increases on oxidation from 2.523(2) Å in **1**·2C<sub>6</sub>H<sub>6</sub><sup>20</sup> to 2.530(2) Å in **3**·2THF, indicating perhaps a slight decrease in the bond strength.

Despite many attempts, single crystals of **4** suitable for X-ray study have not been acquired. It would be interesting to see whether oxidation has the same effect on W–L bond length when a  $\pi$ -conjugated ligand, such as 4-*tert*-butylpyridine, is bonded to the cluster.

**Magnetic Properties.** Magnetic susceptibility data were collected for **3** and **4** with the expectation of paramagnetic behavior due to the one unpaired electron in the HOMO. Plots of corrected  $\chi$  vs 1/*T* for **3** and **4** are available in the Supporting Information. Indeed, the data follow a Curie–Weiss law ( $\chi(T) = C/(T - \theta) + \chi_0$ ) and indicate paramagnetic behavior for both compounds over the temperature range of 4–300 K. The Curie constants calculated for compounds **3** and **4** from these plots are 0.368 and 0.318 mol<sup>−1</sup> K<sup>−1</sup>, respectively. From these Curie constants, the effective moments per cluster were calculated to be  $\mu_{\text{eff}} = 1.71 \mu_B$  for **3** and  $\mu = 1.60 \mu_B$  for **4**, respectively, which are close to the calculated spin-only magnetic moment,  $\mu = 1.73 \mu_B$  (if *g* = 2 and *S* = 1/2). We attribute the slightly lower observed moment for **4** to the partial degradation of the sample by water or other species during handling. Also from the Curie–Weiss plots, the temperature-independent susceptibilities ( $\chi_0$ ) after diamagnetic corrections were found to be 5.11 × 10<sup>−4</sup> emu/mol for **3** and 9.32 × 10<sup>−4</sup> emu/mol for **4**. The Weiss constants ( $\theta$ ) were very close to zero (<0.1 K) for both compounds, which reflects a weak *intercluster* exchange as expected.

(37) Meyer, H. J.; Corbett, J. D. *Inorg. Chem.* **1991**, *30*, 963–967.

(38) Simon, A.; Schnering, H. G.; Schaefer, H. Z. *Anorg. Allg. Chem.* **1967**, *355*, 295–310.

(39) Imoto, H.; Corbett, J. D. *Inorg. Chem.* **1980**, *19*, 1241–1245.

(36) Friebolin, H.; *Basic One- and Two-Dimensional NMR Spectroscopy*; VCH Publishers: New York, 1993; Chapter 7.

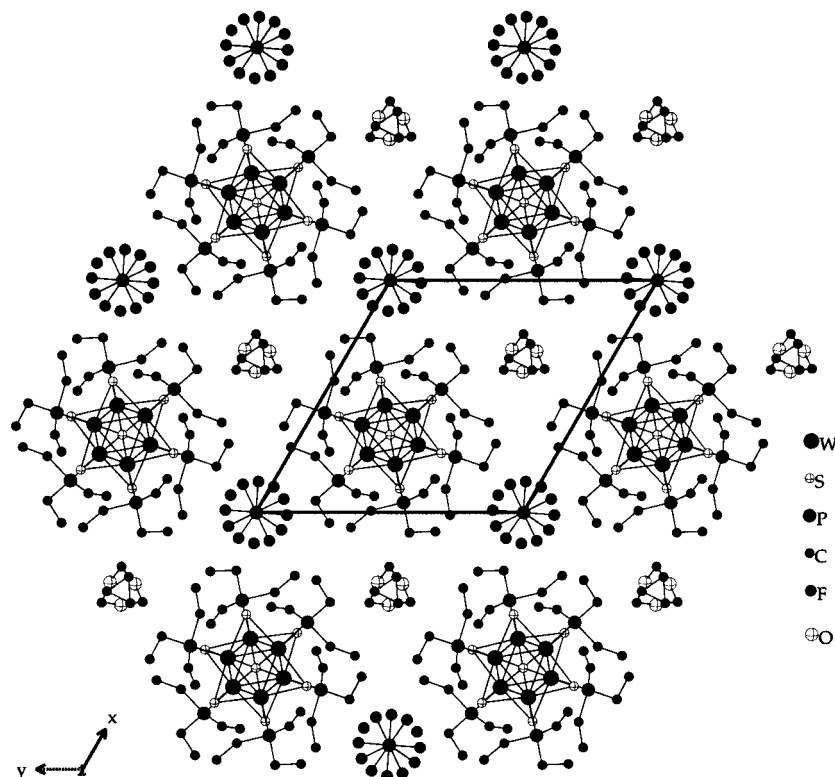


**Figure 3.** View of one layer of  $W_6S_8(PEt_3)_6^+$  ions along the plane  $z = 1/6$  showing the hexagonal arrangement in the crystal structure. The disordered  $PF_6^-$  ions and THF molecules are centered along the planes  $z = 0$  and  $z = 1/12$ , respectively. Additional THF molecules (omitted for clarity) lie directly above the  $PF_6^-$  ions at  $z = 1/4$ .

The ESR spectrum was collected for a powdered sample of **3** at liquid nitrogen temperature. The ESR spectrum, which is available in the Supporting Information, shows a broad signal centered at  $g = 2.04$ . This indicates that **3** contains units with one unpaired electron. The  $21 e^-$  reduced cluster compound  $NaW_6Te_8(\text{pyridine})_6$  was reported to have a  $g$  value of 2.26, measured by ESR.<sup>18</sup>

**Chemical Properties and (In)Stability of the Oxidized Clusters.** The compounds **3** and **4** are fairly stable in the solid state as evidenced by observing the same NMR spectra in solution after the solids were heated under argon at 100 °C for 7 h. However, these compounds display various degrees of “instability” in solution, which are the complicating factors in the syntheses and workup of the oxidized clusters. While the mechanisms and the products of these instabilities are not yet fully understood, some preliminary observations are reported here.

$[W_6S_8(PEt_3)_6]PF_6$  (**3**) is stable in  $CH_2Cl_2$  and THF solutions at room temperature for at least a week as indicated by no change in the appearance of the solutions and no change in the NMR spectra. **3** is stable at 100 °C in  $CH_2Cl_2$  solution for at least 8 h by the same NMR criterion. When **3** is dissolved in acetonitrile or DMF at room temperature, it degrades slowly as indicated by some color change. In some cases, neutral  $W_6S_8(PEt_3)_6$  is formed as evidenced by the  $^1H$  NMR spectra.

Unlike **3**, **4** is quite sensitive. Although in a solution of carefully purified  $CH_2Cl_2$ , **4** appears to be stable for days at room temperature, it undergoes degradation rapidly at a slightly higher temperature (50 °C). Even at room temperature, decomposition occurs in a solution of THF within a few days. The instability of the cluster cation in acetonitrile and DMF is even more dramatic for **4**. After dissolution of **4** in acetonitrile or DMF, the original green solutions change color and some amorphous solid precipitates within minutes. In some cases, the

neutral cluster **2** is formed, but in most cases, whatever is formed from the decomposition is currently beyond our full understanding. This behavior supports the results obtained by cyclic voltammetry which showed  $[W_6S_8(4\text{-}tert\text{-butylpyridine})_6]^+$  to be extremely sensitive to reduction and other reactions in solution, possibly due to impurities such as water or oxygen.<sup>20</sup>

In summary, extreme care must be taken in dealing with solutions of clusters **3** and **4**, especially **4**. The fact that they are generally unstable in DMF and acetonitrile might be attributed to the trace amounts of water and amine impurities, which are common in these solvents and very difficult to eliminate.<sup>40</sup>

**Thermogravimetric Analysis (TGA).** Thermogravimetric analyses were performed on compounds **3** and **4** as indicators of bond strength or lability of the ligands. The TGA traces for **3** and **4** are available in the Supporting Information. The decomposition temperature of **3** (indicated by the onset of the weight loss) is 150 °C, about 100 °C lower than that of the corresponding neutral cluster **1**,<sup>20</sup> but perhaps consistent with a slightly increased W–P distance in **3**. The total weight loss corresponds to the loss of all six ligands. In contrast, the oxidized cluster **4** begins its thermal decomposition at 200 °C, even slightly higher than the neutral  $W_6S_8(4\text{-}tert\text{-butylpyridine})_6$  (190 °C).<sup>20</sup> This may indicate a slightly stronger W–N bond, though a definite conclusion cannot be drawn without a crystal structure. The amount of weight loss corresponds to the loss of approximately five ligands. It is interesting to note that while **4** seems to be significantly more sensitive to decomposition in solution than **3**, the opposite appears to be true with respect to thermal decomposition of the solids.

(40) Perrin, D. D.; Armarego, W. L. F. *Purification of Laboratory Chemicals*, 3rd ed.; Pergamon Press: New York, 1988.

### Conclusions

We have successfully oxidized the  $W_6S_8L_6$  clusters with  $[Cp_2Fe]PF_6$ . The products were studied with NMR spectroscopy, mass spectroscopy, and X-ray crystallography (only for **3**) and are shown to be the desired oxidized  $[W_6S_8L_6]PF_6$  clusters with a MEC of 19. Magnetic property studies showed that they are paramagnetic compounds.

**Acknowledgment.** This work was supported by the Department of Energy (Grant DE-FG02-87ER45298). This work made use of the Polymer Characterization Facility and Electron and Optical Microscopy Facility of the Cornell Center for Materials Research through the National Science Foundation Materials

Research Science and Engineering Centers Program (DMR-0079992). We thank Dr. Mingtao Ge and Prof. Jack Freed for their assistance in collecting the ESR data. We also thank Prof. J. M. J. Fréchet and Mr. Frank Ling for the convenience of the mass spectrometer.

**Supporting Information Available:** ESR spectrum of  $[W_6S_8-(PEt_3)_6]PF_6$ ,  $^{31}P\{^1H\}$  NMR spectra, ESI-MS, plots of  $\chi$  vs  $1/T$ , and thermogravimetric traces of  $[W_6S_8(PEt_3)_6]PF_6$  and  $[W_6S_8(4\text{-}tert\text{-butylpyridine})_6]PF_6$  and X-ray crystallographic file in CIF format for the structure determination of  $[W_6S_8(PEt_3)_6]PF_6 \cdot 2THF$ . This material is available free of charge via the Internet at <http://pubs.acs.org>.

IC001099D